



# Three-Dimensional (3D) Animation and Calculation for the Assessment of Engaging Hill–Sachs Lesions With Computed Tomography 3D Reconstruction

Jimmy Tat, M.D., M.Sc., Jordan Crawford, Jaron Chong, M.D., Tom Powell, M.D., Thomas G. Fevens, Ph.D., Tiberiu Popa, Ph.D., and Paul A. Martineau, M.D.

**Purpose:** To dynamically assess for Hill–Sachs engagement with animated 3-dimensional (3D) shoulder models. **Methods:** We created 3D shoulder models from reconstructed computed tomography (CT) images from a consecutive series of patients with recurrent anterior dislocation. They were divided into 2 groups based on the perceived Hill–Sachs severity. For our cohort of 14 patients with recurrent anterior dislocation, 4 patients had undergone osteoarticular allografting of Hill–Sachs lesions and 10 control patients had undergone CT scanning to quantify bone loss but no treatment for bony pathology. A biomechanical analysis was performed to rotate each 3D model using local coordinate systems to the classical vulnerable position of the shoulder (abduction = 90°, external rotation = 0–135°) and through a functional range. A Hill–Sachs lesion was considered “dynamically” engaging if the angle between the lesion’s long axis and anterior glenoid was parallel. **Results:** In the vulnerable position of the shoulder, none of the Hill–Sachs lesions aligned with the anterior glenoid in any of our patients. However, in our simulated physiological shoulder range, all allograft patients and 70% of controls had positions producing alignment. **Conclusions:** The technique offers a visual representation of an engaging Hill–Sachs using 3D-animated reconstructions with open-source software and CT images. In our series of patients, we found multiple shoulder positions that align the Hill–Sachs and glenoid axes that do not necessarily meet the traditional definition of engagement. Identifying all shoulder positions at risk of “engaging,” in a broader physiological range, may have critical implications toward selecting the appropriate surgical management of bony defects. **Level of Evidence:** level III, case-control study.

Impaction fractures of the posterolateral aspect of the humeral head, referred to as Hill–Sachs lesions, are common sequelae of traumatic anterior glenohumeral joint dislocations.<sup>1</sup> These osseous defects contributed to instability of the joint. In addition, bony Bankarts (glenoid bone defects), either alone or in combination

with the Hill–Sachs lesions, can further compound the instability.<sup>2</sup> It is thought that in a position of athletic function (defined as 90° of abduction combined with external rotation between 0 and 135°), some Hill–Sachs lesions can “engage” with the anterior rim of the glenoid, such that the osseous defect moves over the glenoid rim, leading to possible redislocation.<sup>1,2</sup>

A common approach to clinically assess the risk of engagement is to perform dynamic intraoperative maneuvers during glenohumeral arthroscopy after completion of a Bankart repair.<sup>3</sup> The surgeon will bring the glenohumeral joint into the scapular plane and move the humerus into increasing degrees of abduction and external rotation until the Hill–Sachs is noted to engage or not. More recently, preoperative computed tomography (CT) imaging and 3-dimensional (3D) reconstruction have been used in an attempt to predict engagement.<sup>2,4</sup> In 2007, Yamamoto et al.<sup>4</sup> introduced the glenoid track method, whereby the contact area between the glenoid and the head of the humerus was modeled during shoulder abduction motion under maximal external rotation. If the Hill–Sachs lesion

From the Division of Orthopedic Surgery, University of Toronto, Toronto, Ontario (J.T.); Department of Radiology (J.C., T.P.) and Division of Orthopaedic Surgery (P.A.M.), McGill University Health Centre, Montreal, Quebec, Canada; and Department of Computer Science and Software Engineering, Concordia University, Montreal, Quebec (J.C., T.G.F., T.P.), Canada.

The authors report that they have no conflicts of interest in the authorship and publication of this article. Full ICMJE author disclosure forms are available for this article online, as [supplementary material](#).

Received April 13, 2020; accepted August 6, 2020.

Address correspondence to Jimmy Tat, M.D., M.Sc., University of Toronto, 149 College St., Toronto, ON M5T 1P5. E-mail: [jimmy.tat@mail.utoronto.ca](mailto:jimmy.tat@mail.utoronto.ca)

© 2020 THE AUTHORS. Published by Elsevier Inc. on behalf of the Arthroscopy Association of North America. This is an open access article under the CC BY-NC-ND license (<http://creativecommons.org/licenses/by-nc-nd/4.0/>). 2666-061X/20526

<https://doi.org/10.1016/j.asmr.2020.08.012>

passed outside the margins of the contact area it was considered an “off-track lesion” with the potential to engage.<sup>2,4</sup> In another study, Burns et al.<sup>5</sup> showed that obtaining CT imaging of the shoulder in at risk shoulder positions (60° of glenohumeral abduction and 90° of external rotation), also can help to depict the relative position and interaction of glenoid and humeral bone defects to predict engaging Hill–Sachs. This technique had good agreement with the glenoid track method and sought to improve accessibility in the clinical setting. While these offer a convenient and noninvasive approach, there are discrepancies compared with clinical evaluation with arthroscopy, and it remains unclear how to best predict engaging lesions.<sup>6,7</sup>

Preoperative assessments of engaging Hill–Sachs that are based on size of bone loss, location and orientation of the lesion, and/or the extent of concomitant glenoid bone loss rely on a static criterion, and there is a need for dynamic techniques.<sup>8,9</sup> We therefore created a working moveable 3D CT model that allows the user to move the shoulder joint into various positions to assess the relationship between the Hill–Sachs lesion and the anterior glenoid rim. Our primary goal was to provide an approach to calculate the angle between Hill–Sachs and glenoid rim to identify shoulder positions that could be at risk of engagement.

The purpose was to dynamically assess for Hill–Sachs engagement with animated 3D-shoulder models. We hypothesized that patients having undergone allografting would have a greater number of shoulder positions that would engage compared with the control patients.

## Methods

### Patient Population

With institutional research ethics approval (McGill University Health Centre Research Ethics Board, #2017-2689), we identified retrospectively from the senior author’s (P.A.M.) database consecutive patients with recurrent anterior dislocations. Our 14 patients were divided into 2 groups based on the perceived Hill–Sachs severity. More specifically, they were divided into 4 patients who underwent osteoarticular allografting of the Hill–Sachs lesion versus 10 patients who underwent no specific treatment to address bone loss.

Of the 4 consecutive cases of patients with recurrent anterior shoulder instability who underwent an osteoarticular allografting Hill–Sachs surgery with a primary or revision open Bankart procedure, these cases had undergone humeral allografting based on clinical examination and interpretation of bone loss on CT scan. As controls, we then identified from the same period and from the same database all patients with recurrent shoulder instability (10 total) who had required additional investigation, specifically a CT scan, to assess for

**Table 1.** Patient Demographics and Clinical Information

Characteristic	Allograft	Controls	P Value
	(n = 4)	(n = 10)	
Age, y	27.7 ± 15.9	24.5 ± 4.8	.52
Sex, male/female	4/0	9/1	.51
Shoulder, right/left	2/2	5/5	1.00
Size of Hill–Sachs, mm			
Length	22.2 ± 4.9	18.1 ± 6.8	.28
Width	20.7 ± 6.9	19.9 ± 8.4	.94
Depth	6.7 ± 0.9	5.3 ± 2.8	.35
Glenoid			
Bone loss, % of glenoid	5.0 ± 5.7%	6.8 ± 4.6%	.39
Bony Bankart, y/n	2/2	8/2	.27
Fragment width, mm	1.7 ± 1.9	4.1 ± 3.0	.15
Fragment length, mm	6.9 ± 7.9	11.6 ± 8.3	.35
Fragment size, % of glenoid	2.7 ± 3.1%	4.9 ± 4.3%	.39
Angle of anterior glenoid line*	2.1 ± 3.3°	4.1 ± 3.5°	.25

NOTE. Bone loss = (area of glenoid circle fit loss – area fragment) / glenoid area \* 100%.

bone loss = (area of glenoid circle fit loss – area fragment) / glenoid area \* 100%

\*Angle of anterior glenoid line relative to long axis of glenoid.

bone loss. These patients were identified as having potentially significant bone defects on clinical examination and/or magnetic resonance imaging and subsequently underwent preoperative CT scan for bone loss quantification. Control patients underwent standard arthroscopic Bankart repair without any specific treatment of their bony defects by the senior author (P.A.M.). Patient demographic and clinical information can be found in Table 1. Our study included a range of Hill–Sachs lesion sizes that included mild, moderate, to severe sizes according to the traditional definition that was based on defect dimensions; however, we did not use this classification to categorize patients.<sup>10</sup> As per the glenoid, all subjects in the allograft group had a bony Bankart fragment, and in the control group 8 had a bony Bankart fragment whereas the remaining 2 had no injury to the glenoid.

### Image Acquisition

Full-resolution DICOM (Digital Imaging and Communications in Medicine) sets of axial images at 0.625 mm thickness/0.0 mm separation were obtained, anonymized, and separated into independent folders and processed using 3D Slicer (Burlington, MA) to construct a 3D polygonal mesh. CT threshold settings were set to between 200 and 4000 Hounsfield units to isolate bone from soft tissue. The segmented polygonal mesh was then exported into a stereolithography (\*.stl) format for import into an open-source 3D animation program, Blender (Amsterdam, Netherlands). The static isosurface was duplicated within Blender and independent meshes of the shoulder girdle and the humerus were created.

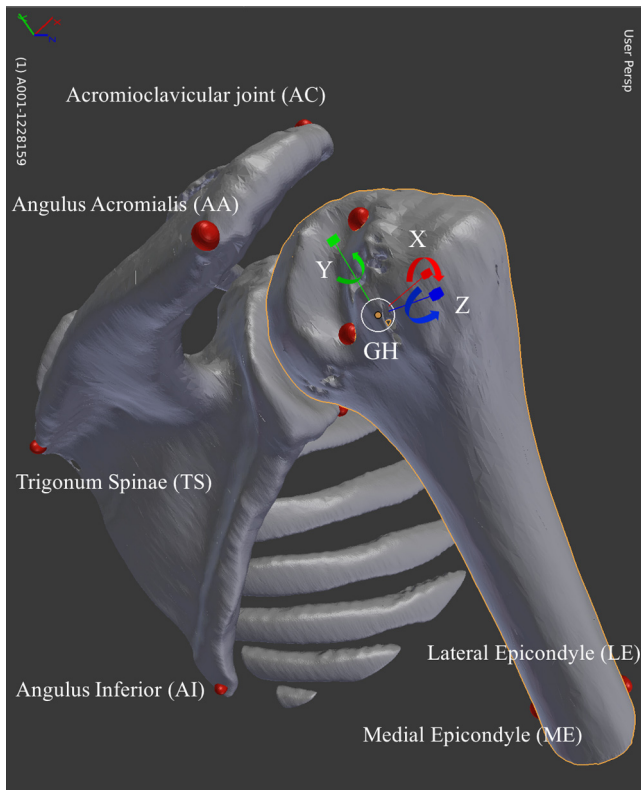


**Fig 1.** Local coordinate system for the humerus and scapula. Spherical markers are placed over bony landmarks of the scapula (AC, AA, TS, AI), and over positions that approximate the humerus (ME, LE). GH represents the glenohumeral center of rotation. The x-axis (red axis) and red arrow show a positive rotation about the x-axis that represents adduction. A positive rotation is also shown about the x-axis (blue axis, blue arrow) showing a flexion moment, and y-axis (green axis, green arrow) showing internal rotation. (AA, angulus acromialis; AC, acromioclavicular joint; AI, angulus inferior; GH, glenohumeral; LE, lateral epicondyle; ME, medial epicondyle; TS, trigonum spinae.)

### Biomechanical Coordinate System

Anatomic local coordinate systems were embedded in each model, according to the International Biomechanics Society convention, to standardize our description of shoulder motion.<sup>11</sup> A local coordinate system was created at the scapula using the following bony landmarks (Fig 1): (1) AC: The most dorsal point on the acromioclavicular joint; (2) TS: trigonum spinae, a point at the medial border in line with the scapular spine; (3) AI: angulus inferior, the most distal point of the scapula; and (4) AA: angulus acromialis, a sharp corner at the dorsolateral side of the scapular spine.

Another local coordinate system was generated for the humerus using the glenohumeral (GH) center of rotation, medial epicondyle, and lateral epicondyle (Fig 1). To estimate the GH center of rotation, we used the sphere-fitting method.<sup>12</sup> The centroid of the articular surface of the humeral head was calculated using a least squares

sense, with 5 data points measured on the surface of the humeral head (Eq. 1 and Eq. 2).<sup>13</sup> We used the location of the centroid as the center of rotation of the humerus in our model in Blender. Since our CT images did not always have the distal aspect of the humerus, we needed to approximate the medial epicondyle and lateral epicondyle to the most distal portion along the humeral shaft on the medial and lateral aspect respectively. We then normalized our humeral coordinate system by mathematically aligning it to scapular coordinate system. Thus, in our study, we describe motion of the humerus with respect to the scapula.

$$J = \sum_{i=1}^n e_i^2 \quad (1)$$

where

$$e_i = \sqrt{(x_i - R_x)^2 + (x_i - R_y)^2 + (x_i - R_z)^2} \quad (2)$$

With the estimated parameters,  $r$  being radius, and  $R_x$ ,  $R_y$ ,  $R_z$  the coordinates of the rotation center of the humerus. The standardization of shoulder motion by the International Biomechanics Society is designed for the right shoulder. Since we had 2 left shoulders, we needed to mirror the raw polygonal mesh with respect to the sagittal plane ( $z = -z$ ), so that we could apply the definitions for the right shoulder.<sup>10</sup> This step was done before defining any landmarks or local coordinate systems.

The Hill–Sachs defect was represented as a unit vector that was created using 2 points in the deepest portion of the Hill–Sachs trough that ran through its long axis (Fig 2). For the glenoid axis, normally it is defined as the most anterior edge of the glenoid, that is parallel to the long-axis of the ellipsoid-shaped glenoid; however, with an osseous injury to the glenoid (bony

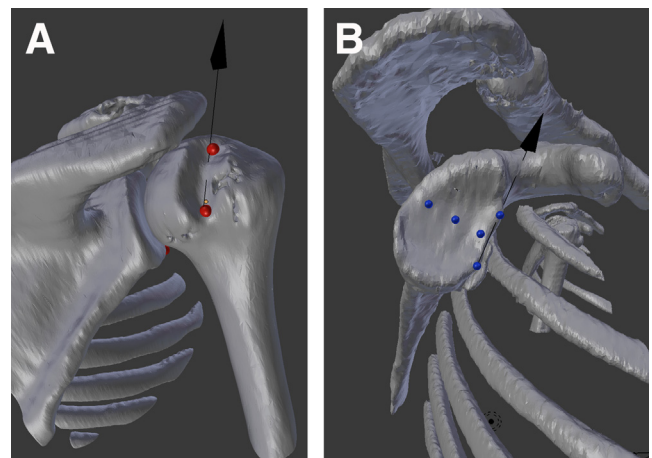


**Fig 2.** (A) Vector position in the trough of a Hill–Sachs lesion. (B) Anterior osseous glenoid defect secondary to previous traumatic injury. Anterior edge of glenoid is defined in this example relative to the true anterior edge and not the long-axis of the articular surface. A vector is cast through this anterior edge.

**Table 2.** Hill–Sachs and Glenoid Angle Through Athletic Function Range (Abduction 90° and ER 0–135°)

Group		Axis			Hill–Sachs Glenoid Minimum Angle, °
		x	z	y	
Allograft	1	–90	0	–55	36.2
	2	–90	0	–35	63.2
	3	–90	0	–35	67.2
	4	–90	0	–45	61.0
Control	1	–90	0	–35	66.5
	2	–90	0	0	71.3
	3	–90	0	–45	44.5
	4	–90	0	–135	63.1
	5	–90	0	–40	21.6
	6	–90	0	0	44.3
	7	–90	0	0	71.7
	8	–90	0	–60	47.1
	9	–90	0	–25	12.4
	10	–90	0	0	91.8

NOTE. x represents (+) adduction and (–) abduction in degrees.  
 z represents (+) flexion and (–) extension in degrees.  
 y represents (+) internal rotation and (–) external rotation in degrees.  
 ER, external rotation.

glenoid deficiency), we used 2 points placed most anterosuperior and anteroinferior edges of the glenoid (Fig 2).

**Definition of Engagement**

The definition used for an “engaging” Hill–Sachs defect was that of Burkhart and De Beer<sup>1</sup> in which the long axis of the Hill–Sachs defect was parallel to the anterior glenoid, so that the Hill–Sachs engages the anterior rim of the glenoid. This should occur in a

position of athletic function, defined as 90° of abduction, with external rotation between 0 and 135°.

**Analysis of Engagement**

We wanted to evaluate the possibility of “engagement” in a number of shoulder positions in a functional range of motion, not just one of athletic function. Using a custom-made MATLAB program (The MathWorks, Natick, MA), we mathematically rotated the humerus local coordinate system using a sequence of XZ’Y”, which represented rotations (Fig 1):

X: Rotation around the Xs-axis of the scapula, represents GH abduction / adduction.

Z: Rotation around the rotated Z-axis of the humerus, parallel to the scapula Y–Z plane, represents GH flexion/extension.

Y: Rotation around the twice rotated Yh-axis of the humerus, represents axial rotation.

The XZ’Y” sequence is well established in 3D kinematic analysis of the glenohumeral joint and is known to limit the chance of gimbal lock error.<sup>11,14</sup> In practice, gimbal lock error can produce erroneously large angular changes with small shoulder movements.

For each shoulder position, the Hill–Sachs orientation was determined using the relationship between the Hill–Sachs unit vector relative to the humerus local coordinate system established in the original acquisition image (Eq. 3).

$$[HsH] * [HG] = HsG \tag{3}$$

where [HsG] is Hill–Sachs with respect to global coordinate system, [HsH] is the relationship between the

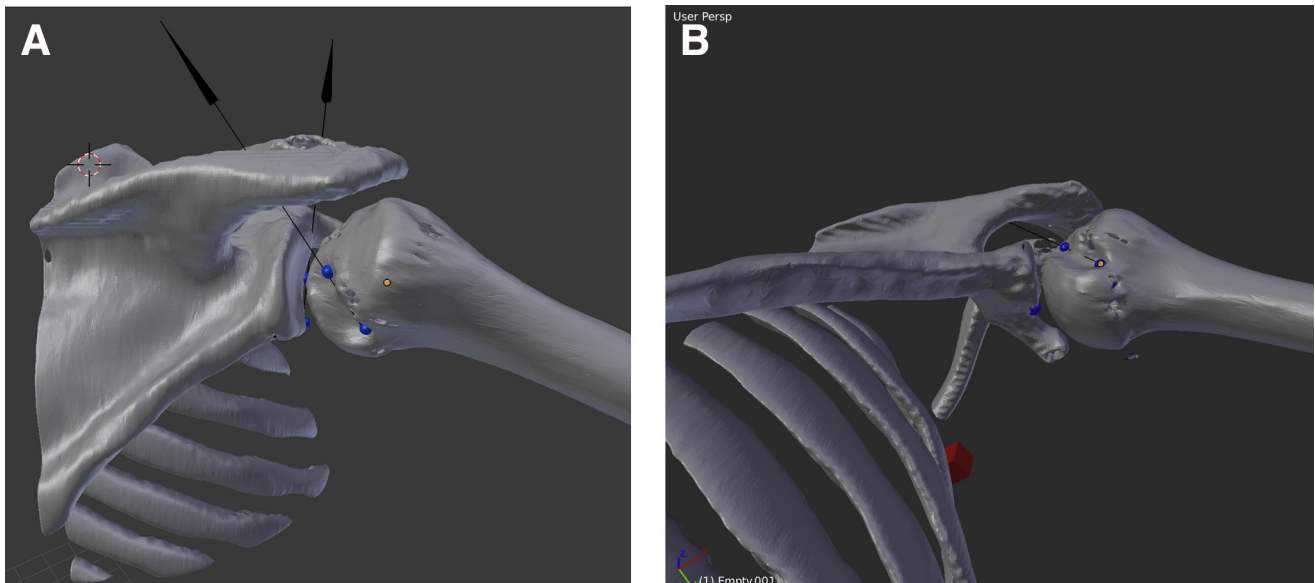


**Fig 3.** Case 1 in a critical position (abduction 90°, flexion 30°, external rotation 135°), (A) posterior view and (B) inferior view, shows an angle of 78.07°. The blue spherical markers were the 2 set of points used to define either the Hill–Sachs and anterior rim of the glenoid, with a connecting arrow between each pair indicating the direction of each vector. The orange dot at the center of the humeral head was the estimated center of rotation for the humerus.

**Table 3.** All Positions with Alignment of Hill–Sachs Axis and Glenoid Axes Per Case

Case	Axis		
	x	z	y
1	-55	-10	-60
	-40	-40	-130
2	-25	-25	-65
	-25	0	-30
	-20	10	-15
	-15	-40	-95
	0	-40	-120
3	-20	-20	-75
	-20	5	-15
	-15	-25	-90
	-5	-30	-120
	0	-30	-135
4	-25	-35	-85
	-25	5	-30
	-10	20	0
	-30	-10	-50

NOTE. x represents (+) adduction and (-) abduction in degrees. z represents (+) flexion and (-) extension in degrees. y represents (+) internal rotation and (-) external rotation in degrees.

Hill–Sachs in relation to the humerus relationship acquired in the original acquisition, and [HG] is the rotated humerus coordinated system. The dot product was then calculated between the Hill–Sachs and glenoid vectors to obtain the angle. An angle of 0 indicated parallel directions and 90° was orthogonal.

Biomechanical functional shoulder range of motion was defined as abduction 0-135° (x-axis), external rotation 0-135° (y-axis), and flexion 0-120° or extension

0-45° (z-axis).<sup>15</sup> Our custom program simulated rotations using 5° increments for each axis in an automated fashion. For example, a rotation sequence might include abduction 90°, flexion 30°, external rotation 90°, and the next increment for the sequence might be abduction 90°, flexion 30°, and external rotation 85°. We tested a total combination of 26,655 shoulder positions. The average computation time in MATLAB per subject was 25.7 ± 2.6 seconds.

We also mathematically rotated the humerus through positions of athletic function and reported the Hill–Sachs and glenoid angles. With the humerus in 90° of abduction, we externally rotated the humerus from 0 to 135°, in 5° increments, and calculated angles at each increment. If an angle of zero was found throughout the range of motion, this represented an engaging Hill–Sachs, according to the definition of Burkhart and De Beer.<sup>1</sup> Conversely, a nonengaging Hill–Sachs has angles greater than zero, throughout the range of motion, in these cases we reported the minimum angle, or angle with the lowest value, that was calculated among all simulated positions.

We compared our allograft group and control groups using Mann–Whitney *U* tests and  $\chi^2$  analysis for nominal data. This included a comparison of patient demographics, Hill–Sachs lesion dimensions, glenoid bone loss dimensions, angle of anterior glenoid line relative to normal axis of glenoid, minimum angle in athletic function, and number of engaging positions in physiological range. Glenoid bone loss was calculated using the surface-area method.<sup>16</sup> Significance was set to a *P* < .05 and all values were presented with means ± standard deviation.

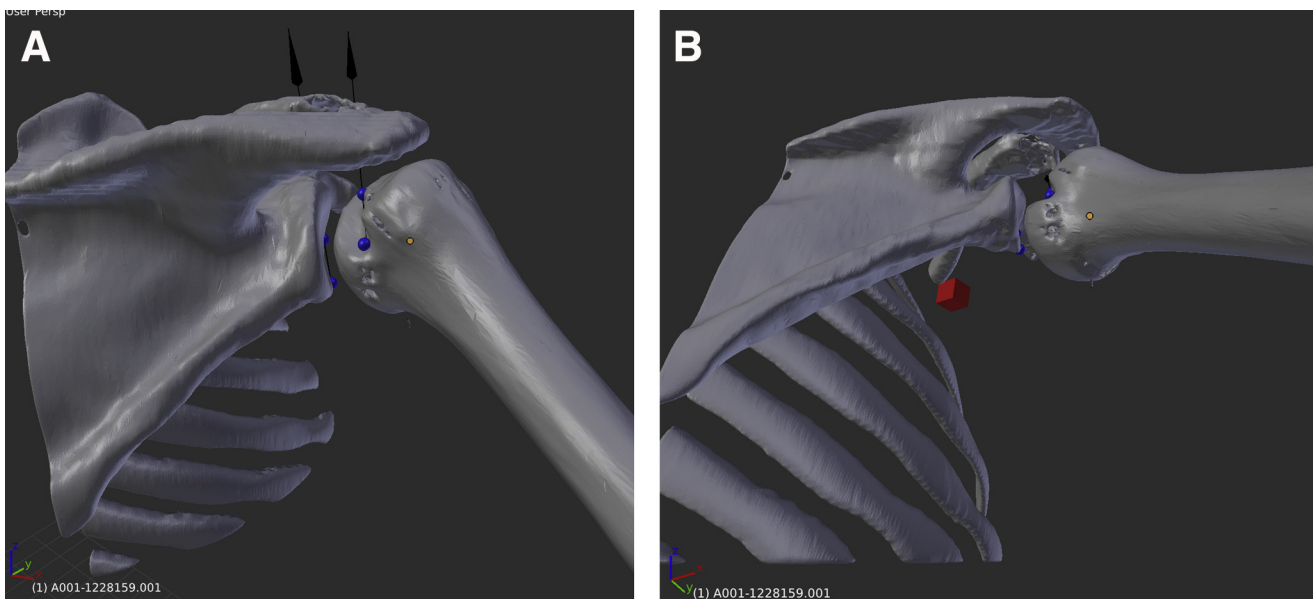


**Fig 4.** Case 1 shoulder with vectors aligned, (A) posterior view and (B) inferior view. The shoulder position (abduction 55°, extension 10°, external rotation 60°) has a parallel Hill–Sachs and anterior glenoid orientation.

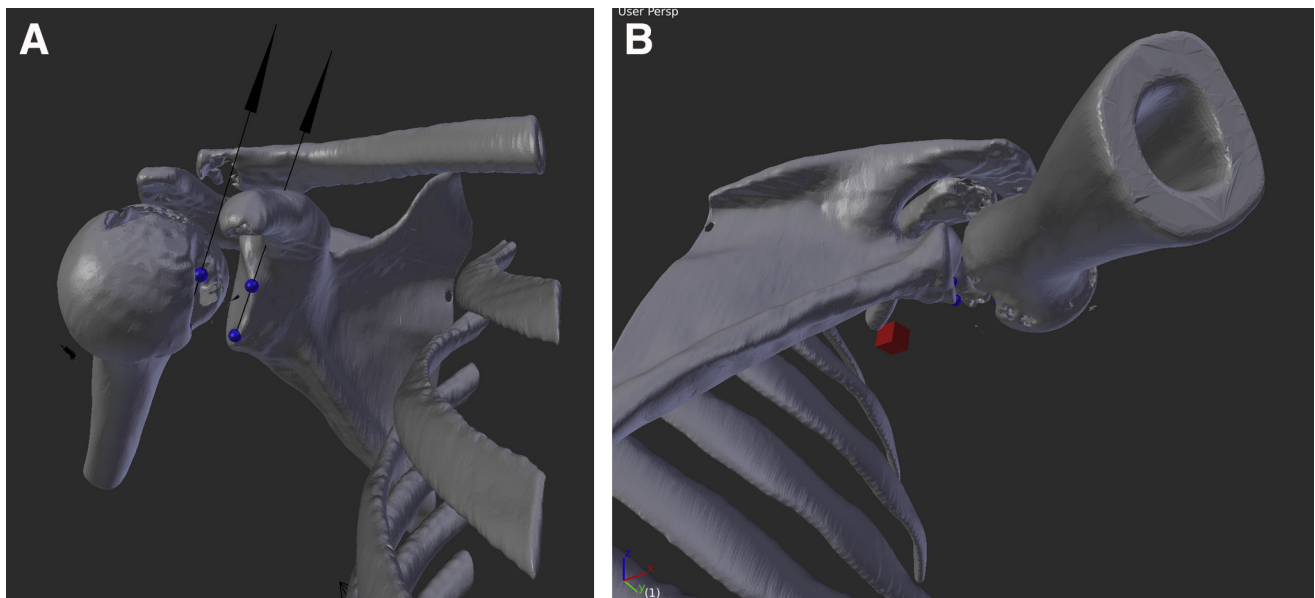


**Fig 5.** Case 1 shoulder with vectors aligned, (A) anterior view and (B) inferior view. The shoulder position (abduction 40°, extension 40°, external rotation 130°) has a parallel Hill–Sachs and anterior glenoid orientation and has no signs of contact between the humeral head and glenoid. Most likely this shoulder position represents one of suprphysiological conditions.

## Results

In positions of athletic function of the shoulder, we did not find the Hill–Sachs lesion to be aligned with the anterior glenoid in any of our cases nor controls. The minimum Hill–Sachs and glenoid angle found through the range of motion are shown in Table 2. We did not find there to be significant differences in the minimum angle achieved in the position of athletic function between our cases and controls (average minimum angle in allograft cases was  $56.9 \pm 14.0^\circ$  and controls was  $53.4 \pm 24.2^\circ$ ,  $P > .99$ ). Using our 3D model, we then moved the humerus through positions of athletic function and demonstrated that there were nonparallel orientations in all cases and controls. In nonparallel orientations, we were able to visualize contact between the articular surface of the humeral head and the glenoid (Fig 3). Therefore, we considered this to be non-engaging and there to be a low risk of engagement in these critical positions, as the nonparallel orientation represents a lack of true articular arc mismatch and is unlikely to produce joint instability.

We then expanded our search and simulated shoulder positions throughout a physiological range of motion for all groups. For our allograft case group, we found that there were multiple shoulder positions, within our functional range, that could produce alignment between the Hill–Sachs and glenoid shown in Table 3. Interestingly, these shoulder positions are not found within a position of athletic function established by Burkhart and De Beer.<sup>1</sup> Again, in our model, we rotated the humerus to the corresponding shoulder positions. In these positions, we observed no additional

points of contact in the remainder of the humeral head, suggesting a position at high risk for “engagement” (Figs 4 and 5).

In our control group, we found there were 3 cases that produced no alignment between the Hill–Sachs and glenoid axes and therefore indicate no position that could engage (Table 4). This could be due to a combination of the defect size being insufficient to cause engagement or the defect location and orientation. In the other 7 controls, interestingly, we found at least 1 shoulder position that could produce alignment. Likewise, these shoulder positions seemed to fall outside the range of athletic function defined by Burkhart and De Beer.<sup>1</sup>

We found that the allograft group had a greater number of positions that would engage (mean  $4 \pm 1$  positions of engagement) compared to our controls (mean  $2 \pm 2$  positions of engagement,  $P = .06$ ).

## Discussion

We developed a method to evaluate the risk of engagement between a Hill–Sachs defect and the anterior glenoid rim. We are able to find all shoulder positions in which the axis of the Hill–Sachs lesion aligns with the axis of the anterior glenoid, and we are able to visualize and animate the relationship between the Hill–Sachs and glenoid in our 3D model. This approach takes into account the dynamic component of shoulder motion instead of relying on static criteria such as the size of the Hill–Sachs and the location of the defect. It also accounts for cases in which bone loss is present on either the humeral or glenoid side or both

**Table 4.** Controls

Controls	Axis		
	x	z	y
1	-20	-15	-50
	-5	-35	-80
2		None	
3	-50	-20	-50
	-15	15	-5
4		None	
5	-85	-25	-45
	-75	-15	-40
	-35	10	-10
6	-50	-30	0
	-35	-35	-25
	-20	-35	-50
	-5	-30	-75
7	0	-25	-85
	0	70	-100
8	-45	-40	-100
	-45	-15	-65
9	-80	-10	-30
	-75	5	-20
	-65	20	-5
	-60	25	0
10		none	

NOTE. x represents (+) adduction and (-) abduction in degrees.  
z represents (+) flexion and (-) extension in degrees.

sides of the joint. We believe that the method presented here is more functionally accurate and provides a clinically relevant approach to the assessment of the overall significance of a Hill-Sachs and bipolar defects.

The technique demonstrated in this cohort study of patients with Hill-Sachs defects found that in the classic positions of athletic function simulated in our model, none of the cases nor controls engaged. However, interestingly, when expanding our simulation to a complete physiological range, we were able to identify multiple shoulder positions that align the Hill-Sachs axis and glenoid axis. For example, in Figure 4, the shoulder is in a position of abduction 55°, extension 10°, external rotation 60°, and shows a parallel orientation between the Hill-Sachs and glenoid axes; however, it falls outside of a position of athletic function. According to the traditional definition of engagement, a Hill-Sachs that aligns in a position less than 70° of abduction and/or in extension, is nonengaging, given it is a “nonfunctional” position.<sup>1</sup> However, we believe the classic definition of a functional position and engagement may oversimplify and underestimate the contribution of bony defects to glenohumeral instability. The same can be said of the glenoid track concept, which also was modeled a path along the humeral in various degrees of abduction but always in maximal external rotation.<sup>7</sup>

Nevertheless, it is well established that to complete activities of daily living a person requires a range 120° of forward flexion, 45° of extension, 130° of abduction,

and 60° of external rotation.<sup>15,17</sup> Thus, we propose that if one can align the 2 axes, then there would be an articular arc mismatch, and we would expect symptoms of instability. If this position occurs outside of the traditional position of athletic function and takes place in a submaximal range that can affect day-to-day tasks there is value in identifying such positions. In addition, many athletic endeavors are routinely performed with the arms in a range of positions outside the traditional description of athletic function. Therefore, our findings may challenge the actual definition of engagement or at the very least warrant a broadening of the description. We do not claim to doubt the classic conceptual definition of engagement, but we merely introduce a technique that accounts for the dynamic component of shoulder motion, and in doing so, avoid limitations of a static criteria assumed traditional definition (like size and location of lesion).

A 3D-animated paradigm provides a means to dynamically and noninvasively visualize the patient's anatomy and determine the clinical significance of a Hill-Sachs lesion and bipolar lesions that can be highly relevant to both the patient as well as the orthopedic surgeon. In this study, our allograft case patients had multiple shoulder positions that could engage. Therefore, we found our biomechanical assessment to be consistent with our intraoperative findings, which demonstrated an engaging Hill-Sachs for patients in the osteoarticular allograft group. However, it was unexpected for us to find that 70% of our controls also had at least one shoulder position that could engage. If these positions correlated with symptoms of shoulder instability, these patients may in fact benefit from surgical intervention specifically addressing the bony defects. However, given our retrospective study design, we were not able to match these high-risk shoulder positions to physical findings of shoulder instability. The next step would be to correlate our findings to the physical examination. Although we expected to find at least one position when a Hill-Sachs was made, some of controls had no position. It is then possible that the Hill-Sachs was created in supraphysiological range outside what the local coordinate system will allow. If this is the case, then these lesions truly do not have any chance of physiological engagement.

### Limitations

Our study also was limited by our small sample size of 4 cases and 10 controls. This may limit the generalizability of our results. However, we think the sample was appropriate for the goal of our work, which was to introduce a technique for assessing engagement of Hill-Sachs lesions. Furthermore, the patients in our allograft case group represented a subset of patients with recognized severe bony defects having been designated to require a complex surgery with greater

potential morbidity for successfully treating the instability. Similarly, our control group also was generated from a subset of patients with some amount of bone loss, since they represented all patients during the same period who required additional imaging in the form of the CT scan to better define the bony pathology noted on the magnetic resonance imaging arthrogram and suggested on clinical examination. Lastly, our biomechanical model describes rotation of the glenohumeral joint alone; it does not include glenohumeral translation or scapulothoracic motion that may occur in the shoulder.

### Conclusions

The technique offers a visual representation of an engaging Hill–Sachs using 3D-animated reconstructions with open-source software and CT images. In our series of patients, we found multiple shoulder positions that align the Hill–Sachs and glenoid axes that do not necessarily meet the traditional definition of engagement. Identifying all shoulder positions at risk of “engaging,” in a broader physiological range, may have critical implications towards selecting the appropriate surgical management of bony defects.

### References

- Burkhart SS, De Beer JF. Traumatic glenohumeral bone defects and their relationship to failure of arthroscopic Bankart repairs: Significance of the inverted-pear glenoid and the humeral engaging Hill–Sachs lesion. *Arthroscopy* 2000;16:677-694.
- Di Giacomo G, Itoi E, Burkhart SS. Evolving concept of bipolar bone loss and the Hill-Sachs lesion: From “engaging/non-engaging” lesion to “on-track/off-track” lesion. *Arthroscopy* 2014;30:90-98.
- Provencher MT, Frank RM, LeClere LE, et al. The Hill–Sachs lesion: Diagnosis, classification, and management. *J Am Acad Orthop Surg* 2012;20:242-252.
- Yamamoto N, Itoi E, Abe H, et al. Contact between the glenoid and the humeral head in abduction, external rotation, and horizontal extension: A new concept of glenoid track. *J Shoulder Elbow Surg* 2007;16:649-656.
- Burns DM, Chahal J, Shahrokhi S, et al. Diagnosis of engaging bipolar bone defects in the shoulder using 2-dimensional computed tomography: A cadaveric study. *Am J Sports Med* 2016;44:2771-2777.
- Khoury V, Van Lancker HP, Martineau PA. Sonography as a tool for identifying engaging Hill–Sachs lesions preliminary experience. *J Ultrasound Med* 2013;32:1653-1657.
- Metzger PD, Barlow B, Leonardelli D, et al. Clinical application of the “Glenoid track” concept for defining humeral head engagement in anterior shoulder instability a preliminary report. *Orthop J Sports Med* 2013;1:2325967113496213.
- Bollier MJ, Arciero R. Management of glenoid and humeral bone loss. *Sports Med Arthosc Rev* 2000;18:140-148.
- Fox JA, Sanchez A, Zajac TJ, et al. Understanding the Hill-Sachs lesion in its role in patients with recurrent anterior shoulder instability. *Curr Rev Musculoskelet Med* 2017;10:469-479.
- Rowe CR, Zarins B, Ciullo JV. Recurrent anterior dislocation of the shoulder after surgical repair. Apparent causes of failure and treatment. *J Bone Joint Surg Am* 1984;66:159-168.
- Wu G, Van der Helm FC, Veeger HD, et al. ISB recommendation on definitions of joint coordinate systems of various joints for the reporting of human joint motion—Part II: Shoulder, elbow, wrist and hand. *J Biomech* 2005;38:981-992.
- Meskers CG, Van der Helm FC, Rozendaal LA, et al. In vivo estimation of the glenohumeral joint rotation center from scapular bony landmarks by linear regression. *J Biomech* 1997;31:93-96.
- Van der Helm FC, Veeger HE, Pronk GM, et al. Geometry parameters for musculoskeletal modelling of the shoulder system. *J Biomech* 1992;25:129-144.
- Šenk M, Cheze L. Rotation sequence as an important factor in shoulder kinematics. *Clin Biomech* 2006;21:S3-S8.
- Doorenbosch CA, Harlaar J, Veeger DH. The globe system: an unambiguous description of shoulder positions in daily life movements. *J Rehabil Res Dev* 2003;40:147.
- Sugaya H, Moriishi J, Dohi M, et al. Glenoid rim morphology in recurrent anterior glenohumeral instability. *J Bone Joint Surg Am* 2003;85:878-884.
- Rundquist PJ, Obrecht C, Woodruff L. Three-dimensional shoulder kinematics to complete activities of daily living. *Am J Phys Med Rehabil* 2009;88:623-629.